Fingering Instability of Spinning Drops

F. Melo, J. F. Joanny,[a] and S. Fauve
Ecole Normale Supérieure de Lyon, 46, Allée d'Italie, 69364 Lyon, France
(Received 16 June 1989)

We report a study of a fingering instability which occurs during the spreading of a spinning drop. We measure the time evolution of the drop profile, the critical radius for instability onset, and the fastest growing instability wavelength. The experimental results are compatible with the predictions of lubrication theory when the centrifugal effect is not too large compared to the capillary one.

PACS numbers: 47.20.Dr, 68.15.+e, 68.45.Gd

Studies of the dynamics of interfaces between two domains have been performed in various fields of physics and much progress has been made in the understanding of unifying ideas.[1] Widely studied experimental situations concern viscous fingering and crystal growth; another class of phenomena is associated with wetting dynamics, i.e., motion of contact lines where two fluids and a solid substrate meet.[2] The forced motion of a straight or circular contact line is known to be unstable to the formation of fingers in a direction perpendicular to the main flow; typical examples include the flow a thin viscous fluid layer down an inclined plane,[3,4] and the spreading of a rotating drop.[5] We report in this Letter a study of this last experimental situation, used for industrial purposes to generate liquid films of well controlled thickness and known as spin coating. When a drop of viscous fluid is released on a rotating horizontal solid surface, it rapidly takes up a circular form, with a radius increasing with time under the action of the centrifugal force. The film profile is flat around the center but presents a rim with a strong maximum near the contact line [see Fig. 1(b)]. At later times, waves of increasing amplitude develop along the rim, as seen in Figs. 1(c) and 1(d), and break into fingers as displayed in Figs. 1(e) and 1(f). We show that the time evolution of the film thickness is not affected by the instability and follows a simple scaling law. When the centrifugal effect is not too large compared to the capillary one, we find that the predictions of lubrication theory, i.e., the existence of a critical radius for instability onset and the development of a given number of fingers independent of the experimental parameters, are compatible with the experimental results. We discuss the deviations from these laws observed at high rotation rates.

Our experimental setup consists of a horizontal rotating disk of radius 5 cm, driven by a variable-speed motor at a rotation frequency f, in the range 3–80 Hz, with velocity fluctuations less than 2%. Vibrations produced by the motor are damped by the coupling with the disk, reducing the fluctuations from horizontal to less than 5×10^{-4} rad. The substrates are silicon wafers from the electronics industry, polished on one side and covered with a thin layer of natural oxide. The fluids used are silicon oils, that completely wet the silicon substrate. The drop is placed on the center of the disk with a syringe with a precision in volume of 0.5 μl. Its position with respect to the center is controlled to about 0.1 mm using an X-Y precision displacement. The drop is placed on a slowly rotating substrate. At a given instant the rotation velocity is rapidly increased, driving a radial spreading of the liquid. The liquid film is illuminated with a stroboscope, synchronized to the rotating disk with a photodiode, in order to stabilize the orientation of the successive images recorded on a video apparatus through a semitransparent mirror.

The nonzero-slope regions of the liquid film reflect the incident parallel light beam, and thus produce black zones on the photographs displayed in Figs. 1(a)–1(f). In the early stages, the circular spreading of the drop is stable, as shown in Figs. 1(a) and 1(b). The drop profile is first approximately flat, and the height of the film decreases in the vicinity of the contact line [see Fig. 1(a)]. A bump then develops in the vicinity of the rim of the drop, its maximum height being visualized by a bright annulus clearly visible in Fig. 1(b). Then, small-amplitude waves spontaneously develop and modulate the rim. The wave amplitude and the drop mean radius increase in time but the instability angular wavelength remains constant [see Figs. 1(c)–1(e)]. Wavy modulations of the contact line are associated with modulations of the rim profile in a direction perpendicular to the main flow, thus producing a capillary pressure gradient in this direction. As shown recently,[6] this is the basic instability mechanism for liquid films driven by an external force, the main condition being the existence of a bump in the profile. The capillary pressure gradient induces a secondary flow that generates the small drops, visible in Fig. 1(e) near the contact line, which give rise to fingers [see Fig. 1(f)]. Let us notice that this instability can be suppressed when the drop is released on a surface prewetted by a thick enough film of the same silicon oil.

We have first investigated the time evolution of the drop radius, R, and of the film thickness, h. The experimental parameters are the disk rotation angular velocity ω, the fluid density ρ, the drop volume Ω, the fluid viscosity η, and the surface tension γ. With these parameters and h, r, and t, we can define five independent dimensionless variables, for instance, h/H_0, r/R_0, t/T_0,

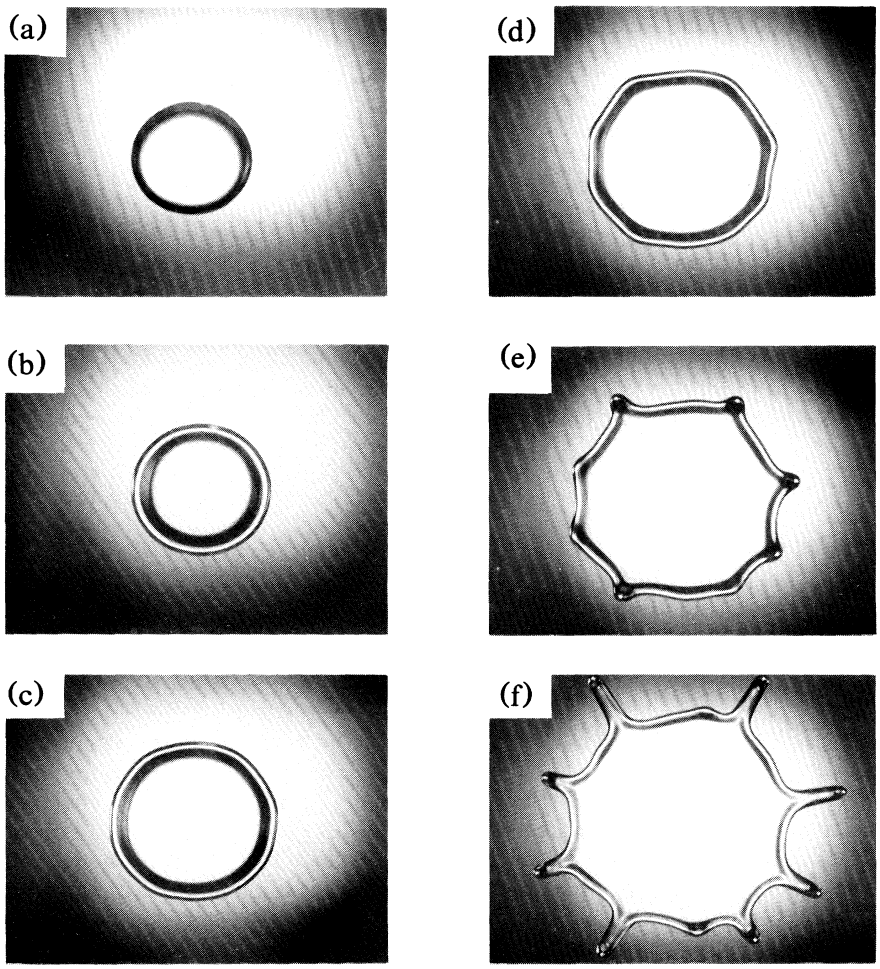

FIG. 1. The different stages of spreading of a spinning drop. The black zones correspond to the nonzero-slope regions of the liquid film. (a) Initial conditions; a volume of 50 μl of silicon oil (viscosity 50 cm^2/s) is released on the substrate, rotating at a frequency $f=10$ Hz. (b) After 30 s; formation of a bump, visualized by the bright annulus, in the vicinity of the contact line. (c) After 140 s; the wavy modulation of the rim at the early stage of instability. (d) After 180 s; development of the wavy perturbation. (e) After 220 s; break up into fingers. (f) After 310 s; well developed fingering.

β, and ωt, where the characteristic scales H_0, R_0, and T_0 are defined below. The dimensionless parameter β is analogous to an inverse Bond number, $\beta=\gamma/\rho\omega^2\Omega$, and measures the competition between capillary and centrifugal effects; ωt measures the ratio between the centrifugal force and the Coriolis force, which is negligible whenever $\omega t \gg 1$. Dimensional arguments imply that R/R_0 evolves in the following way [$h(R,t)\approx 0$ (Ref. 7)]:

$$R/R_0 = f(t/T_0,\beta)\,. \tag{1}$$

In order to determine the characteristic scales, we use the lubrication approximation; the spreading equation reads

$$3\eta\mathbf{U} = h^2(\rho\omega^2\mathbf{r}+\gamma\boldsymbol{\nabla}\boldsymbol{\nabla}^2 h)\,, \tag{2}$$

where $\mathbf{r}=(r,\theta)$ are polar coordinates. In the derivation of Eq. (2), both the hydrostatic pressure contribution due to the gravity and the Coriolis force are neglected, and the local curvature is approximated by $\boldsymbol{\nabla}^2 h$ (in the limit where $\partial h/\partial r \ll 1$). The height profile is obtained from the continuity equation,

$$\frac{\partial h}{\partial t}+\boldsymbol{\nabla}\cdot\left[\frac{h^3}{3\eta}(\rho\omega^2\mathbf{r}+\gamma\boldsymbol{\nabla}\boldsymbol{\nabla}^2 h)\right]=0\,. \tag{3}$$

Equation (3) traces back to the volume conservation; for a circular drop of radius $R(t)$ and volume Ω, its integral form reads

$$\int_0^{R(t)} 2\pi r h(r,t)\,dr = \Omega\,. \tag{4}$$

All parameters of Eq. (3) can be absorbed in the follow-

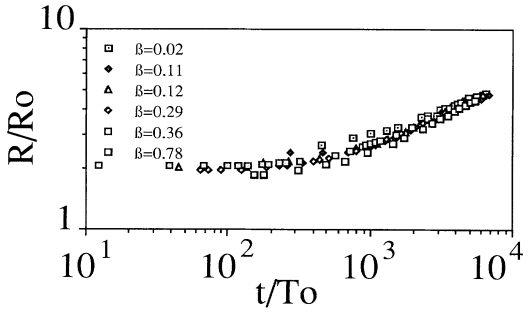

FIG. 2. Dimensionless radius R/R_0 of the drop as a function of the dimensionless time t/T_0. Initial conditions are important at short times, while the evolution of the radius is universal at long times in the explored parameter range.

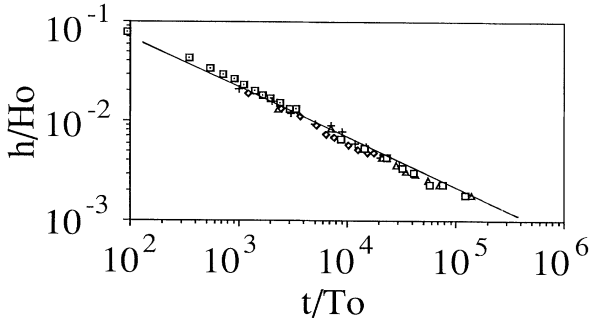

FIG. 3. Dimensionless film thickness h/H_0 in the central region, as a function of the dimensionless time t/T_0. The straight line is the theoretical prediction obtained from Eq. (7). The experimental data correspond to the following values of ν, f, and Ω in cgs units: (⊡) 50, 2, 0.1; (+) 100, 5, 0.1; (△) 100, 9, 0.1; (◇) 50, 5, 0.07; (□) 50, 9, 0.07.

ing scaling:[8]

$$h=H_0\xi, \quad (r,\theta)=(R_0\chi,\theta), \quad t=T_0\tau, \tag{5}$$

with

$$R_0=\Omega^{1/3}\beta^{1/6}, \quad H_0=\Omega^{1/3}\beta^{-1/3}, \quad T_0=\Omega^{1/3}\beta^{5/3}\eta/\gamma.$$

Equation (3) becomes

$$\frac{\partial\xi}{\partial\tau}+\nabla\cdot[\xi^3(\chi+\nabla\nabla^2\xi)]=0; \tag{6}$$

Eq. (6) implies that the dimensionless radius of the drop must be a function of the dimensionless time only. Moreover, in the central region, the profile is flat and the curvature term can be neglected; starting from a flat profile $h=h_0$ at the initial instant, the methods of characteristics gives the solution at long times,[9]

$$\frac{1}{\xi^2}-\frac{1}{\xi_0^2}=\frac{4\tau}{3}. \tag{7}$$

The memory of initial conditions is lost for dimensionless times larger than $1/\xi_0^2$, and an asymptotic regime is reached where h decreases as $t^{-1/2}$ and R increases as $t^{1/4}$.

The experimental results displayed in Fig. 2 show that, when the drop radius is normalized with respect to R_0 and the time with respect to T_0, all the experimental data indeed collapse on a single curve, as expected from Eq. (1). We have also measured the film thickness h at the center as a function of time. Small particles placed on the solid substrate and on the liquid free surface are focused with a microscope, and allow film-height measurements with a precision of about 5 μm. The rotation is stopped for a short time to make the measurements. Silicon oils of very high viscosity are used in order to increase the relaxation time of the drop. The results plotted in Fig. 3 show that, when the dimensionless parameters h/H_0 and t/T_0 are used, the data collapse on a line for all values of the parameters η, ω, and Ω. Its constant slope indicates that the film thickness decreases like $t^{-0.5}$, in agreement with the prediction of Eq. (7), and is independent of the fingering instability. The above experimental results imply that large-curvature effects near the contact line (β small), and Coriolis force effects (ωt small), are negligible for the time evolution of R in the explored parameter range.

In the vicinity of the contact line, there is a small region where capillary pressure must be taken into account. Its size l is given by balancing the capillary and centrifugal terms of Eq. (2) around $r=R$; we get $l=(\gamma\Omega/\rho\omega^2R^3)^{1/3}$. It is shown in Ref. 6 that the film profile has a maximum within a distance of order 1 from the contact line, and decays to the flat profile predicted by Eq. (7) toward the center. This is clearly visible on the photographs of Figs. 1(b)–1(f), where the rim size is found to be roughly $5l$.

As the spreading proceeds, the rim develops waves that modulate the contact line and the rim profile in a direction perpendicular to the main flow; these wavy perturbations are noticeable in Fig. 1(c) and increase in amplitude with a constant angular wavelength [see Fig.

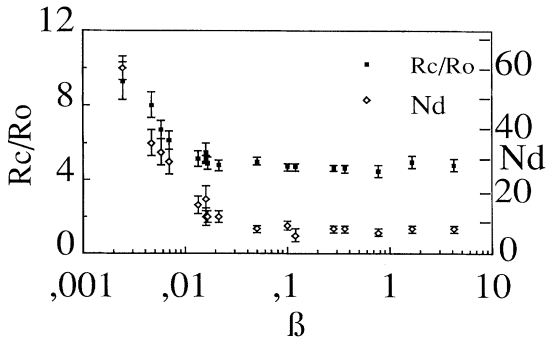

FIG. 4. The dimensionless critical radius R_c/R_0, and the number of fingers N, as a function of $\beta=\gamma/\rho\omega^2\Omega$. When β is not too small, R_c/R_0 and N are constant, in agreement with the predictions of the lubrication theory.

1(d)]. The instability mechanism traces back to the capillary pressure gradients induced by the modulation of the rim profile that drive a secondary flow in a direction perpendicular to the main flow.[6] Equation (7) shows that the dimensionless critical radius for the instability onset, as well as the unstable wavelength, i.e., the number of fingers, is a function of β only (neglecting the Coriolis force); in the lubrication approximation these are constants independent of β as shown by Eq. (5). This is observed experimentally for $\beta > 0.01$ (see Fig. 4). For smaller values of β, the dimensionless critical radius and the number of unstable fingers increases. We conclude that the lubrication approximation is not valid when β is too small (for instance, when the rotation speed is too large). Indeed, using the Tanner law to estimate the dynamic contact angle Θ gives $\Theta \propto (\eta U/\gamma)^{1/3} \propto \beta^{-1/2}$, which shows that large-curvature corrections must be taken into account when β is small ($\Theta \gg 1$). These involve to leading order terms proportional to β^{-1} that must be added to Eq. (5), and the dimensionless critical radius and wavelength therefore depend on β when β is too small.

The development of the instability consists of fluid accumulation and formation of small drops along the rim under the action of the capillary pressure gradients [see Fig. 1(e)]. These drops then give rise to fingers, the tip positions of which move like $t^{0.65}$, while the central-part radius increases roughly like $t^{0.3}$. A rough estimation can be made from the time evolution of the film thickness, $h \propto t^{-1/2}$, and volume conservation. We obtain an increase of the central-part radius as $t^{1/4}$ and, assuming that the fingers grow roughly with a constant width, and that the flow from the central part is negligible, a growth of the finger size as $t^{1/2}$. More precise estimations would require a better knowledge of the time evolution of the profile, particularly in the vicinity of the drop rim.

A natural extension of the present work involves a similar study in the case of drops spreading in a Hele-Shaw cell, with or without fluid injection at the center. On the theoretical side, it would be interesting to derive from (5) the reduced equation governing the motion of the drop rim, considered as a moving interface.

We are grateful to the Centre National d'Etudes des Télécommunications (Meylan) for providing the silicon wafers used in these experiments.

---

[a]Permanent address: Institut Charles Sadron, 6, rue Boussingault, 67083 Strasbourg CEDEX, France.

[1]See, for instance, *Dynamics of Curved Fronts,* edited by P. Pelcé, Perspectives in Physics (Academic, New York, 1988).

[2]P. G. de Gennes, Rev. Mod. Phys. **57**, 827 (1985).

[3]H. E. Huppert, Nature (London) **300**, 427 (1982).

[4]N. Silvi and E. B. Dussan, Phys. Fluids **28**, 5 (1985).

[5]L. H. Tanner, La Recherche **17**, 184 (1986).

[6]S. M. Troian, S. A. Safran, E. Herbolzheimer, and J. F. Joanny, Europhys. Lett. (to be published).

[7]A singularity arises at the contact line because of the no-slip condition; the profile h must be matched to the precursor film, or a region with slip must be considered in the vicinity of the contact line (see, for instance, the review of Ref. 2).

[8]A similar argument has been used for the flow of a thin viscous fluid layer down an inclined plane, L. W. Schwartz, Phys. Fluids A **1**, 443 (1989).

[9]J. F. Joanny, thesis, University of Paris 6, 1985 (unpublished).

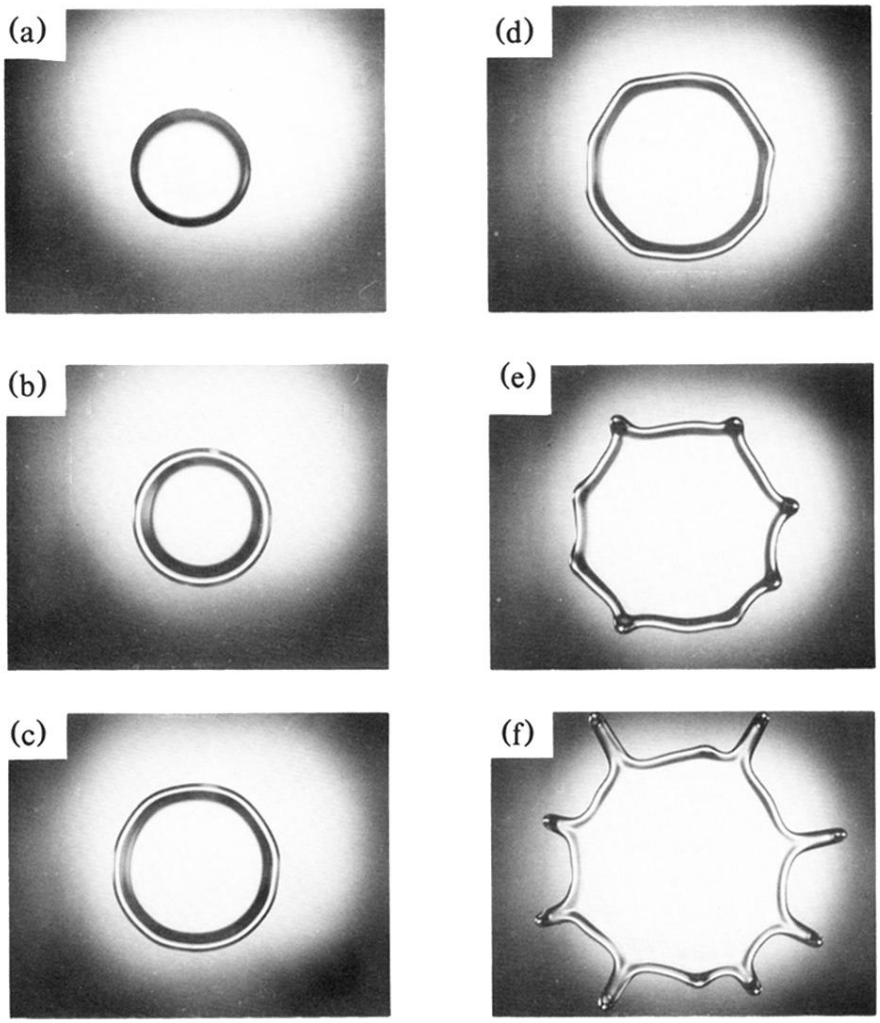

FIG. 1. The different stages of spreading of a spinning drop. The black zones correspond to the nonzero-slope regions of the liquid film. (a) Initial conditions; a volume of 50 μl of silicon oil (viscosity 50 cm^2/s) is released on the substrate, rotating at a frequency $f = 10$ Hz. (b) After 30 s; formation of a bump, visualized by the bright annulus, in the vicinity of the contact line. (c) After 140 s; the wavy modulation of the rim at the early stage of instability. (d) After 180 s; development of the wavy perturbation. (e) After 220 s; break up into fingers. (f) After 310 s; well developed fingering.